

# Viscoelastic Dewetting of Constrained Polymer Thin Films

SYLVAIN GABRIELE,<sup>1</sup> PASCAL DAMMAN,<sup>1</sup> SÉVERINE SCLAVONS,<sup>1</sup> SYLVAIN DESPREZ,<sup>1</sup> SÉVERINE COPPÉE,<sup>1</sup> GÜNTER REITER,<sup>2</sup> MOUSTAFA HAMIEH,<sup>2,3</sup> SAMER AL AKHRASS,<sup>2</sup> THOMAS VILMIN,<sup>4</sup> ELIE RAPHAËL<sup>4</sup>

<sup>1</sup>Laboratoire de Physicochimie des Polymères, Université de Mons Hainaut, 20, Place du Parc, B-7000 Mons, Belgium

<sup>2</sup>Institut de Chimie des Surfaces et Interfaces, Unité Propre de Recherche du Centre National de la Recherche Scientifique (UPR9069), 15, Rue Jean Starcky, B.P. 2488, 68057 Mulhouse Cedex, France

<sup>3</sup>Laboratoire de Chimie Analytique, Matériaux, Surfaces et Interfaces, Département de Chimie, Faculté des Sciences I, Université Libanaise, Hadeth, Beyrouth, Liban

<sup>4</sup>Laboratoire de Physico-Chimie Théorique, Unité Mixte de Recherche du Centre National de la Recherche Scientifique 7083, Ecole Supérieure de Physique et Chimie Industrielle, 10 Rue Vauquelin, F-75231 Paris Cedex 05, France

Received 21 November 2005; revised 16 May 2006; accepted 1 June 2006

DOI: 10.1002/polb.20919

Published online in Wiley InterScience (www.interscience.wiley.com).

**ABSTRACT:** Thin films of fluids are playing a leading role in countless natural and industrial processes. Here we study the stability and dewetting dynamics of viscoelastic polymer thin films. The dewetting of polystyrene close to the glass transition reveals unexpected features: asymmetric rims collecting the dewetted liquid and logarithmic growth laws that we explain by considering the nonlinear velocity dependence of friction at the fluid/solid interface and by evoking residual stresses within the film. Systematically varying the time so that films were stored below the glass-transition temperature, we studied simultaneously the probability for film rupture and the dewetting dynamics at early stages. Both approaches proved independently the significance of residual stresses arising from the fast solvent evaporation associated with the spin-coating process. © 2006 Wiley Periodicals, Inc. *J Polym Sci Part B: Polym Phys* 44: 3022–3030, 2006

**Keywords:** dewetting instability; interfaces; polystyrene; thin films; viscoelasticity

## INTRODUCTION

Thin liquid films are ubiquitous in everyday life, in which they play leading roles in lubrication, protective coatings, countless natural and industrial processes, and so forth.<sup>1</sup> In addition, with the development of modern technologies, functional devices of progressively smaller and smaller sizes are required. It is thus not surprising that under such conditions the thickness of polymer films has reached values even smaller than the diameter of the unperturbed molecule.

Understanding polymer thin-film stability represents several challenges: On the one hand, the causes for the rupture of thin films are not yet fully identified even for simple fluids, not to speak of highly viscoelastic polymers that could exhibit additional elastic instability.<sup>2</sup> On the other hand, the influence of the confinement of chainlike molecules on film stability and polymer dynamics has not been clearly elucidated.<sup>3,4</sup> Numerous studies have demonstrated clear deviations from bulk behavior. Unfortunately, despite enormous efforts over the last decade,<sup>4,5</sup> our understanding of the origin of several puzzling properties of such thin films is still not satisfactory. As a possible origin of these unexpected properties, the conditions of film preparation have been identified<sup>3,6–8</sup> because they can lead to polymer chains that are not in their

Correspondence to: P. Damman (E-mail: pascal.damman@umh.ac.be), G. Reiter (E-mail: g.reiter@uha.fr), or E. Raphaël (E-mail: elie.rafael@espci.fr)

*Journal of Polymer Science: Part B: Polymer Physics*, Vol. 44, 3022–3030 (2006)  
© 2006 Wiley Periodicals, Inc.

equilibrium state. Physical properties of such thin films, such as the density, may thus change over the course of time. It is still unclear if film preparation has direct consequences with respect to the stability and dynamics of such films. It may be anticipated that nonequilibrium chain conformations cause residual stresses in spin-coated polymer thin films.

The aim of this article is to provide some insight into the origin of the puzzling properties of polystyrene (PS) thin films. We show that the atypical dewetting dynamics and the probability for film rupture can be attributed to nonlinear friction at the fluid/substrate interface and residual stresses caused by the way the films have been prepared.

## DEWETTING BASICS

A thin film of a liquid deposited on a nonwetable, solid surface is not stable when it is thinner than the critical thickness,  $h_c = \kappa^{-1} \sin(\theta/2)$ , where  $\theta$  and  $\kappa^{-1}$  are the contact angle and the capillary length, respectively [ $\kappa^{-1}$  is defined by the surface tension of the liquid ( $\gamma$ ), its density ( $\rho$ ), and the acceleration due to gravity  $g$  through the relation  $\kappa^{-1} = (\gamma/\rho g)^{1/2}$ ].<sup>1</sup> If the fluid has enough mobility, dewetting may occur, and holes (dry patches) and edge retraction can thus be observed. The system gradually evolves toward its equilibrium state, which corresponds to a collection of droplets on the solid substrate, these droplets being characterized by the equilibrium contact angle ( $\theta$ ). To achieve this equilibrium state, different successive processes are involved: the initial rupture of the film, the opening (retraction) dynamics of holes (edges), and a Rayleigh–Plateau instability of the rims collecting the dewetted fluid.<sup>9,10</sup>

Initiated by the stimulating work of Brochard-Wyart and coworkers,<sup>11–13</sup> experimental and theoretical studies of thin-film dewetting have allowed us to extract principal scaling laws based on a simple energetic approach. It relies on the assumption that the viscous dissipation inside a film can be smaller than the dissipation due to the friction at the interface between the film and the substrate. The observation of several dewetting dynamics has been explained by the slippage of the polymer at the solid surface.<sup>13</sup> This wall slip is usually characterized by the hydrodynamic extrapolation length [or slippage length ( $b$ )], which is defined as the distance from the wall at which the interfacial velocity ( $V_{\text{slip}}$ ) extrapolates to zero:<sup>14</sup>  $b = \eta/\zeta$  [where  $\eta$  is the

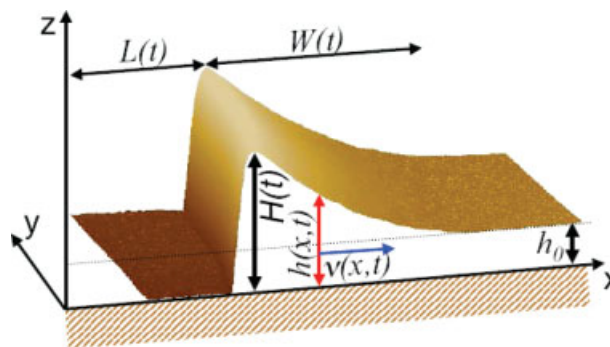


**Figure 1.** Film geometry observed by AFM.  $h(x,t)$  is the profile of the film,  $h_0$  is the initial height of the film,  $H(t)$  is the height of the front,  $L(t)$  is the dewetted distance,  $W(t)$  is the width of the rim, and  $v(x,t)$  is the velocity of the film. [Color figure can be viewed in the online issue, which is available at [www.interscience.wiley.com](http://www.interscience.wiley.com).]

viscosity of the liquid and  $\zeta$  is the friction coefficient related to a linear interfacial force (per unit of the surface) of the liquid onto the substrate,  $F_f = \zeta V_{\text{slip}}$ .<sup>14–16</sup> It has been predicted that the  $b$  value of a polymer liquid on a flat and passive substrate can be given by the relation  $b = a(N^3/P^2)$  (where  $a$  is the monomer size,  $N$  is the polymerization index, and  $P$  is the entanglement index).<sup>14</sup>

For viscoelastic polymers such as PS, stress propagation in films of initial thickness  $h_0$  is limited to a characteristic length,  $\Delta = (h_0 b)^{1/2}$ , because of the interfacial friction and elasticity.<sup>13</sup> For a hole radius ( $d$ ) smaller than  $\Delta$ , the dissipation of the capillary energy,  $|S|$  (where  $S = \gamma_{\text{sv}} - \gamma_{\text{sl}} - \gamma$  is the spreading parameter, which is negative for nonwetable substrates;  $\gamma_{\text{sv}}$  and  $\gamma_{\text{sl}}$  are the surface free energy of the solid vapor and solid liquid interfaces, respectively), essentially occurs within the fluid. Then, the opening dynamics are exponential ( $d \sim e^{t/\tau}$ , where  $\tau$  is the relaxation time), and no rim can be detected. For larger hole diameters such as  $\Delta < d$ , dissipation at the solid/fluid interface dominates. The birth of a rim is observed with a characteristic rim width ( $W$ ) proportional to  $\Delta$  and a constant dewetting velocity of  $V = (S/\zeta)\Delta^{-1}$ . At later stages, in the mature rim regime [dewetted distance ( $L$ )  $> b$  and  $W$  much larger than  $\Delta$ ],  $W$  and the height of the rim ( $H$ ) can be obtained with volume conservation:  $W \sim L h_0 / (H - h_0)$ , which gives the relation  $W \sim H \sim L^{1/2}$  (see Fig. 1). In this regime,  $V$  decreases with time  $t$  according to  $V \sim t^{-1/3}$ , giving the classical law  $d \sim t^{2/3}$ , which usually is used to infer dewetting with strong slippage.<sup>15,16</sup>

In the absence of a solid or liquid substrate (e.g., hole opening in a freestanding film) the velocity profile within the film corresponds to true plug flow,  $b$  thus becomes infinite, and only the first regime (exponential growth) is observed ( $d$  is always smaller than  $\Delta$ ).<sup>17–19</sup>

## EXPERIMENTAL

For the corresponding experimental studies, we used thin PS films with weight-average molecular weights ( $M_w$ 's) ranging from 35 to 4840 kD and a polydispersity index lower than 1.15.  $h_0$  varied between 20 and 100 nm, as measured by ellipsometry. The films were obtained by the direct spin coating of toluene solutions onto silicon substrates coated with a thin layer of adsorbed polydimethylsiloxane (PDMS) chains ( $M_w = 26$  or 90 kg/mol, layer thickness  $\approx 4$ –6 nm). These irreversibly adsorbed PDMS layers resulted from spin-coated films on hydroxylated silicon wafers (cleaned with UV ozone, plasma, or so-called Piranha solutions), which then were annealed at 150 °C for 5 h *in vacuo*. The isothermal dewetting of thin PS films, that is, the retraction of a straight contact line or the opening of holes, was followed in real time ( $t$ ) by optical microscopy. Images were captured with a charged coupled device (CCD) camera. To determine the shape of the rim somewhat more precisely, additional measurements were performed with atomic force microscopy (AFM) in the tapping mode.

## RESULTS AND DISCUSSION

### Rupture of the Liquid Film

Although it is easy to experimentally observe the formation of dry areas in a fluid film, the physical mechanisms associated with the rupture process have been passionately debated in the literature for many years.<sup>20–23</sup> The nucleation and spinodal rupture of thin films can be deduced from a simple analysis of the evolution of free energy with the thickness.<sup>1</sup> Already in 1966, Vrij<sup>24</sup> proposed a spinodal rupture mechanism with a preferred inter-hole distance. We do not, however, discuss the spinodal rupture in this article and refer to previous articles on that topic.<sup>20,23,25</sup> Instead, we focus on a heterogeneous nucleation mechanism. AFM observations indicate that dust/surface heterogeneities, sometimes observed at the center of the holes, could play a role in initiating the rupture. However, such

dust/heterogeneities can be strongly reduced in number by a careful film preparation method.

Recently, a new concept based on the presence of residual stresses in polymer thin films was proposed as an alternative explanation of the rupture mechanism via heterogeneous nucleation.<sup>6,20</sup> For instance, a 40% reduction of the initial hole nucleation density during annealing at temperatures largely above the glass-transition temperature ( $T_g$ ) was reported by Podzimek et al.<sup>20</sup> More surprisingly, we have found that the probability for film rupture, defined as the maximum number of circular holes ( $N_{\max}$ ) per unit of area formed in a film of given thickness, also depends on the aging time ( $t_{\text{aging}}$ ), the time that the film is stored at temperatures below the glass transition.<sup>6</sup>  $t_{\text{aging}}$  starts from the solvent quench during spin coating. As shown in Figure 2(a), a drastic reduction in the hole density was observed after the films were stored at 50 °C for long times. Plotting  $N_{\max}$  as a function of  $t_{\text{aging}}$  [Fig. 2(b)] indicates an exponential decay,  $N_{\max}(t_{\text{aging}}) = N_{\max}(\infty) + N_{\max}(0) \exp[-t_{\text{aging}}/\kappa(N_{\max})]$ , with a limiting value of  $N_{\max}(\infty) = 3 \pm 1$  and a characteristic decay time of  $\kappa N_{\max} = 47 \pm 6$  h, implying that almost no holes will be formed after the films are aged for extended periods ( $t_{\text{aging}} > \kappa$ ). Some holes, however, may be nucleated by defects such as dust particles.

Rupture can be related to the spin-coating process used to prepare thin polymer films. Because of the rapid solvent evaporation, we can consider that polymer chains are not in their equilibrium conformation (e.g., lack of entanglements).<sup>8</sup> The departure from equilibrium generates residual stresses within the film that could initiate the rupture. A detailed description of the physical mechanism by which residual stress can generate holes in thin films is in preparation.

### Dewetting Dynamics: Friction, Viscoelasticity, and Residual Stress

First observations of dewetting for highly elastic polymer thin films, such as high- $M_w$  PS, reveal the formation of strongly asymmetric rims<sup>26</sup> and unusual dewetting dynamics.<sup>27</sup> Several theoretical models have been proposed to explain the asymmetric rims: viscoelasticity,<sup>28</sup> shear thinning,<sup>29</sup> and strain rate hardening.<sup>30</sup> However, even if these models describe quite well the asymmetric rim shape, they cannot explain all of the observed features, such as the logarithmic dewetting dynamics.<sup>27</sup>

In fact, two of us have recently shown that polymer slippage at the solid surface could explain the

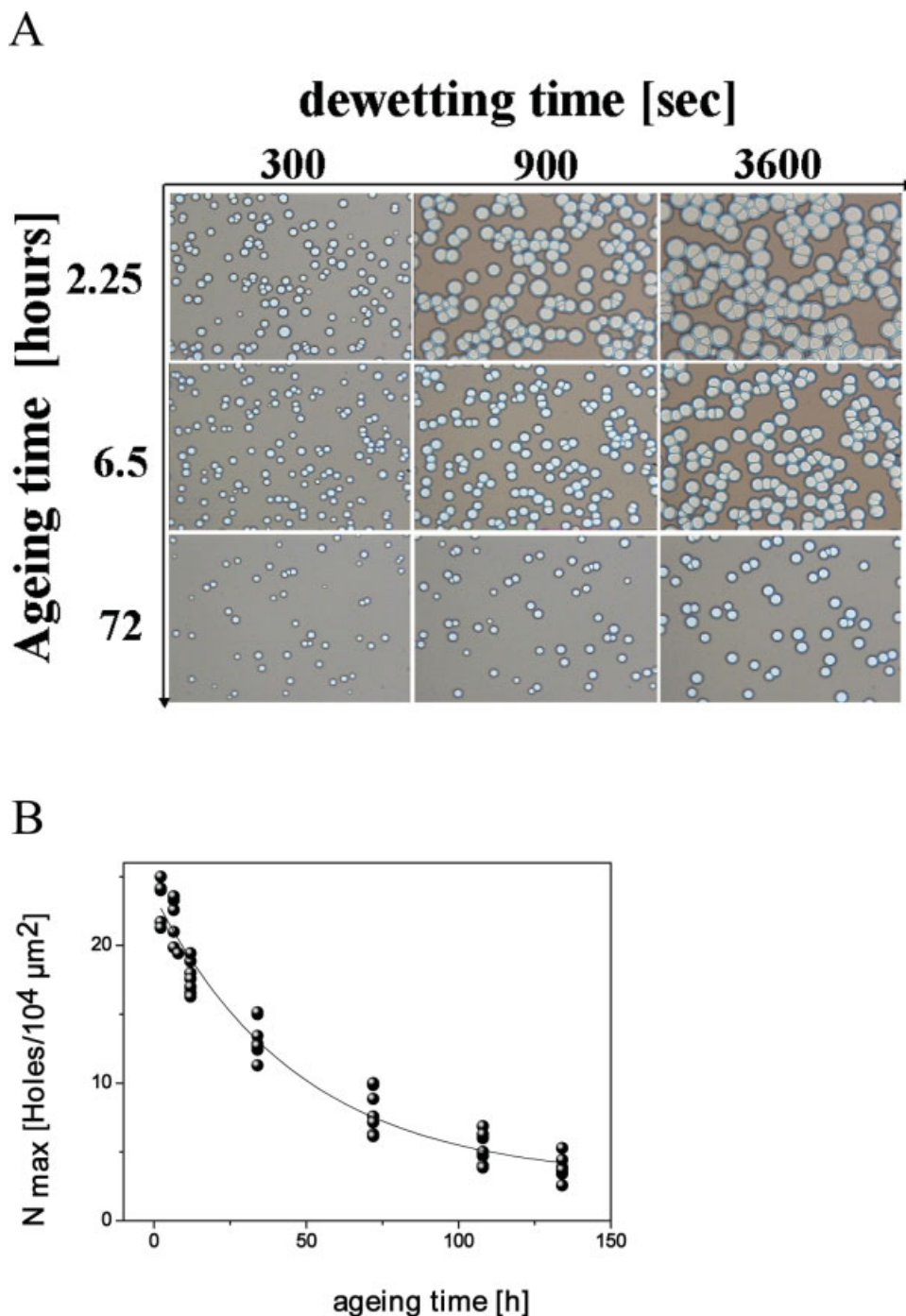


**Figure 2.** (A) Optical micrographs showing the formation of holes in a 40-nm-thick PS film ( $M_w = 4840$  kD) on a PDMS (6 nm) coated Si wafer. The  $X$  and  $Y$  axes represent the time of dewetting at  $125^\circ\text{C}$  and the time of aging, respectively (the films were stored at  $50^\circ\text{C}$ ). The size of the images is  $310 \times 210 \mu\text{m}^2$ . (B) Evolution of  $N_{\max}$  for PS films ( $h_0 = 40$  nm,  $M_w = 4840$  kD) stored at  $50^\circ\text{C}$  for various times. [Color figure can be viewed in the online issue, which is available at [www.interscience.wiley.com](http://www.interscience.wiley.com).]

formation of asymmetric rims.<sup>31</sup> During the early stages of viscoelastic dewetting, the rim shape changes fundamentally. Initially, the energy sup-

plied by the capillary forces is mainly dissipated in the vicinity of the hole edge by viscous losses (due to radial and orthoradial deformations). Under

such conditions, no rim is formed next to the circular dewetted zone. However, as the radius of the hole becomes larger than  $\Delta$  or if the dewetting starts from a straight edge of the sample, the dissipation due to the radial and orthoradial deformations becomes weaker, and the friction at the substrate/film interface gains importance. As a result of this friction, the velocity is damped over distance  $\Delta$  within the film. This results in the appearance of a highly asymmetric rim (Fig. 1), with a steep side reaching a height  $H$  next to the three-phase contact line and an approximately exponential decay on the other side, with a decay length  $\Delta$ .<sup>26,27,31</sup>

Different dewetting dynamics can be directly related to the different rim shapes. In the following, we focus on the asymmetric rim regime.<sup>27</sup> This intermediate regime is rather pronounced for highly viscous thin films close to the glass transition. Our time-resolved experiments (Fig. 3) for dewetting from a straight edge have shown that during these early stages of rim buildup, both  $L$  and  $W$  increase in a logarithmic fashion in time, up to time  $\tau_1$  (the relaxation time of residual stresses), when  $W$  reaches a maximum. Correspondingly, during this stage  $V$  decreases continuously according to a power law,  $V \sim t^{-n}$ . Interestingly, around  $\tau_1$ , the exponent ( $-n$ ) changes from  $-1$  to  $-1/2$  [Fig. 3(C)].<sup>6,27</sup> We want to emphasize that a logarithmic time dependence of  $L$  (and  $W$ ) and the corresponding  $t^{-1}$  decrease of  $V$  are not expected for a Newtonian liquid and that our results cover times shorter than the longest relaxation time in equilibrated bulk samples [i.e., the reptation time ( $\tau_{\text{rep}}$ )]. Thus, the viscoelastic properties of PS certainly affect our dewetting experiments. We have therefore developed a theoretical model that takes into account interfacial friction (i.e., slippage) and viscoelasticity.

A hydrodynamic model within the lubrication approximation including viscoelasticity was recently proposed,<sup>32</sup> but unfortunately this model, limited to small  $b$  values ( $b < h_0$ ), cannot be applied to our experiments, which deal with very large  $b$  values ( $b > h_0$ ). The energetic approach, first proposed by Brochard-Wyart et al.,<sup>13</sup> is most useful when one studies non-Newtonian liquids. However, the viscoelasticity of polymer liquids often brings along great difficulties in solving the flow equations. In the case of the dewetting of thin films, these difficulties can be circumvented as follows. Viscoelastic liquids can be characterized at short times by an elastic modulus ( $G$ ). At times longer than  $\tau$ , it has a Newtonian-like behavior, with  $\eta = \tau G$ .<sup>33</sup> Concerning dewetting,

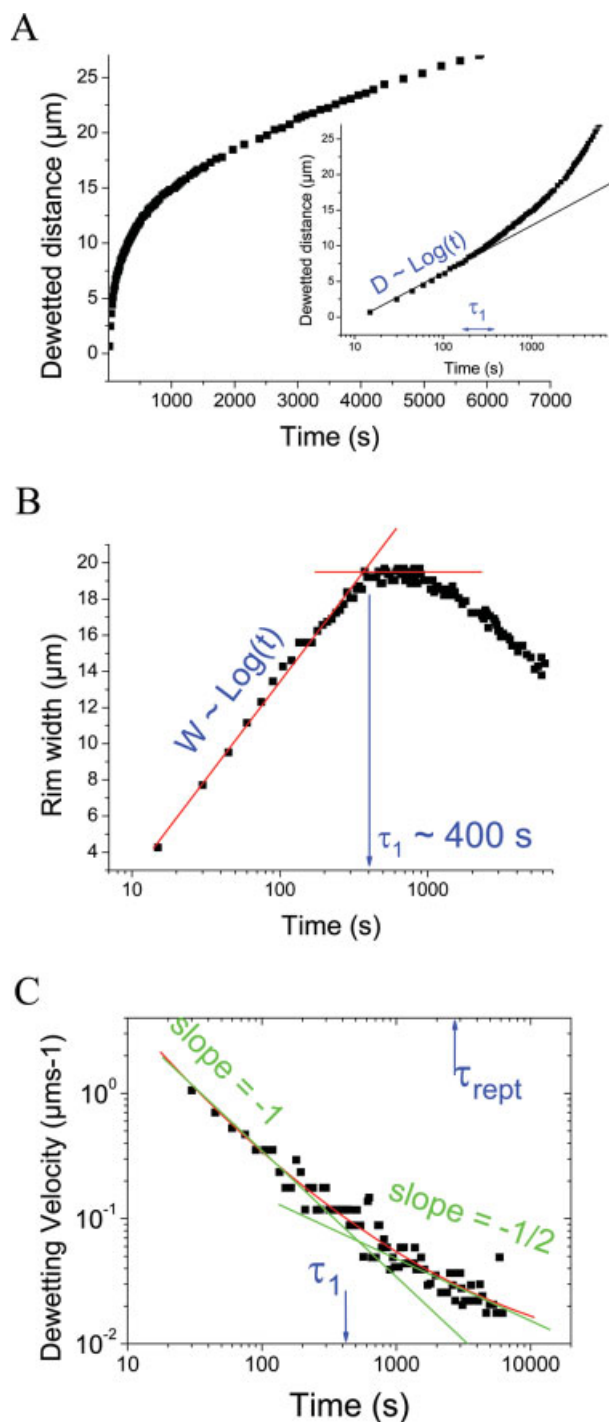


**Figure 3.** (A) Dewetted distance  $L$  (from the straight edge of the sample), (B) rim width  $W$ , and (C) dewetting velocity  $V$  versus time, respectively. The data were obtained for a 65-nm-thick PS ( $M_w = 390$  kg/mol) film dewetted at 140 °C. Characteristic time  $\tau_1$  is indicated. Under the conditions of the experiment, the longest relaxation time of the polymer (its  $\tau_{\text{rep}}$  value) was about 2500 s.

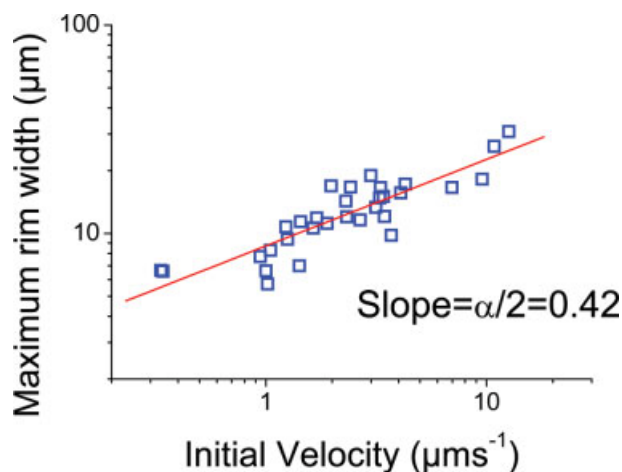


**Figure 4.** Determination of  $\alpha$  from a plot of the maximum rim width versus the initial dewetting velocity for different PS thin films on PDMS-coated silicon wafers. [Color figure can be viewed in the online issue, which is available at [www.interscience.wiley.com](http://www.interscience.wiley.com).]

the result of elasticity is to prevent  $H$  from increasing more than the maximum height of the rim (i.e.,  $H_{\max} = h_0 + |S|/G$ ). This imposes an augmentation of  $W$  during the dewetting process:  $W = Lh_0G/|S|$ . This is associated with a decrease in the velocity such as  $t^{-1/2}$  until  $\tau = \eta/G$  is reached.<sup>31</sup> Interestingly, even in the elastic regime, the dynamics are directly related to the friction process via the increase in  $W$ . The exponent  $-1/2$  for the reduction of the dewetting velocity of an elastic film is thus fully determined by the friction law  $F_f = \zeta V_{\text{slip}}$ .

It is striking to notice that the experiments show a much faster decrease in the velocity, as fast as  $V \sim t^{-1}$ , during the early stage of dewetting ( $t < \tau_1$ ). To explain a more rapid decrease in the dewetting velocity, we have included a nonlinear friction law at the solid/fluid interface. Indeed, several experiments with grafted or adsorbed PDMS surfaces have shown a very weak dependence of the friction force on the sliding velocity (e.g.,  $F_f \sim V^{1/5}$ ).<sup>34,35</sup> Often, substrates that are treated to be flat and passive (for that reason, they are coated with a polymer monolayer) lead to a friction force ( $F_f$ ) that does not depend linearly on the dewetting velocity ( $V$ ) as expected for solid friction.<sup>34</sup> There, we find the following relation:  $F_f \sim V^{(1-\alpha)}$ , where  $\alpha$  is the friction exponent ( $0 < \alpha < 1$ ). For the PS films on PDMS-coated silicon wafers,  $\alpha$ , as determined from a plot of the maximum rim width ( $W_{\max}$ ) versus the initial velocity (Fig. 4), is found to be very close to unity ( $\alpha = 0.84$ ). In contrast, if  $\alpha$  is equal to zero as for solid/solid friction,  $W_{\max}$  does not vary with the initial

dewetting velocity. In Figure 4, a variation of more than 1 order of magnitude can be observed for  $W_{\max}$ . A weakly varying friction force ( $\alpha$  is close to 1) leads to a more rapid decrease in the dewetting velocity:<sup>36</sup>  $V \sim t^{-1/(2-\alpha)} \approx t^{-1}$ . This is consistent with the experimentally observed behavior.

Another mystery about dewetting dynamics, however, remains. As for the initial rupture probability of the films (discussed previously), physical aging at temperatures below  $T_g$  also drastically influences the dewetting dynamics.<sup>6</sup> Figure 5(a) shows that  $W_{\max}$  and the dewetting velocity decrease significantly when the films are aged. Aging can be achieved at very low temperatures, Figure 5(a) shows the drastic influence of the storage time

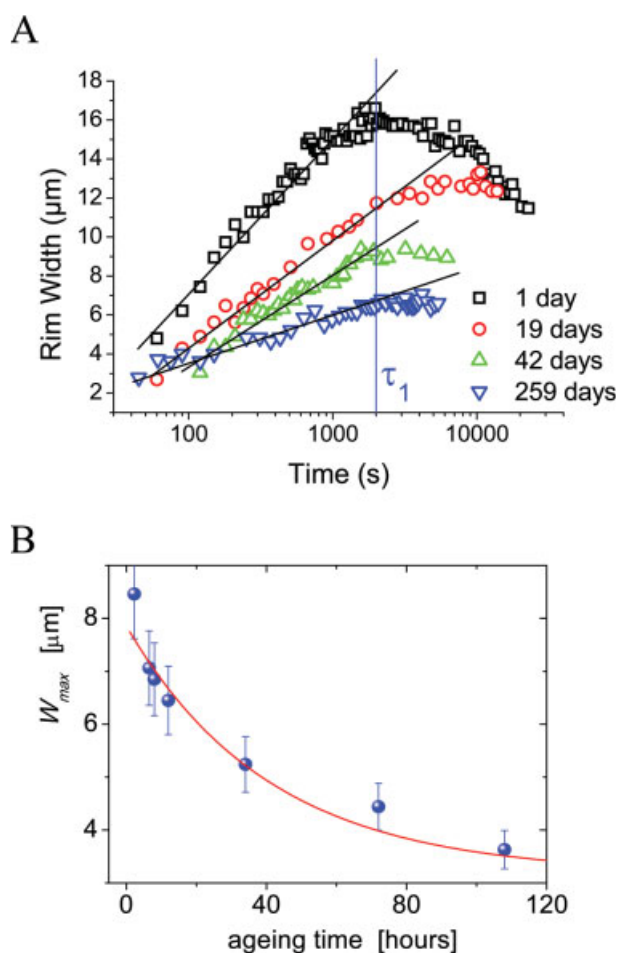


**Figure 5.** (A)  $W$  (for dewetting from the straight edge of the sample) as a function of the dewetting time for films ( $h_0 = 57$  nm,  $M_w = 233$  kD) aged at room temperature for different times.  $W_{\max}$  was reached at about the same time for all the samples. (B) Evolution of  $W_{\max}$  for PS films ( $h_0 = 40$  nm,  $M_w = 4840$  kD) stored at  $50^\circ\text{C}$  for various times. [Color figure can be viewed in the online issue, which is available at [www.interscience.wiley.com](http://www.interscience.wiley.com).]

at room temperature, that is, 75 °C below  $T_g$ , on the formation of the rim (after 42 days,  $W_{\max}$  decreases by a factor of 2). Systematic studies on the temporal evolution of  $W_{\max}$  for films stored at 50 °C, shown in Figure 5(b), indicate an exponential decay of  $W_{\max}$  with  $t_{\text{aging}}$ ,  $W_{\max}(t_{\text{aging}}) = W_{\max}(\infty) + W_{\max}(0) \exp[-t_{\text{aging}}/\kappa W_{\max}]$ , exhibiting a characteristic decay time of  $\kappa W_{\max} = 41 \pm 7$  h, very close to the decay time observed for hole nucleation probability.

The large decrease in the dewetting velocity observed during aging at temperatures well below  $T_g$  of PS can be interpreted by the consideration of either a decrease in the residual stress or a modification (in the course of aging) of the PS/PDMS interface and thus of the friction properties. Theoretically, the contribution of residual stresses to the dewetting dynamics is equivalent to an additional driving force, in parallel to the capillary forces. However, this additional force will decrease during dewetting. Physical aging causes a relaxation of residual stresses and thus a reduction of the driving force, as observed. By combining nonlinear friction and residual stresses ( $\sigma$ ), we can obtain an increase in the initial dewetting velocity by a factor of  $(1 + h_0\sigma/|S|)^{-2/(2-\alpha)}$ .<sup>36</sup> Again, we assume that the fast evaporation of the solvent during spin coating inevitably leads to frozen-in nonequilibrated chain conformations of the polymers. Such nonequilibrated polymer chains generate residual stresses within the film. In the course of aging, or with heating above  $T_g$ , these stresses tend to disappear as the chainlike molecules will adopt conformations closer to their equilibrium.

In that picture, the time characterizing the transition between both dewetting regimes, corresponding to  $W_{\max}$  and a change in the dewetting velocity, can be related to  $\tau_1$ . In a way similar to that proposed in the article of Roth et al.,<sup>19</sup> the transition at  $\tau_1$  can be viewed as a transient time required to reach steady-state flow in the system. The proposed rheological model is used to describe this transient behavior of the polymer. The relaxation of the stress is represented by  $\tau_1$ , which, in turn, is determined by the internal structure (chain conformations) of the film. Later, we show the evolution of this relaxation time with parameters characterizing the polymer (see the Dewetting and Rheology section).

We cannot exclude a modification of the interface during aging. The PDMS coating is made from adsorbed chains on a silicon wafer, the loops and tails being still mobile, that can relax easily and might modify the PDMS/PS interface, even

well below  $T_g$  of PS. This may strongly reduce the slippage and thus the dewetting velocity. Such a modification of the interface remains, however, speculative. Systematic experiments to study the dynamics of PDMS chains at the PDMS/PS interface are in progress.

## Dewetting and Rheology

As shown by several studies, dewetting or hole opening can be considered a rheological investigation of polymer chains in nanometer thin films.<sup>18–20,37,38</sup> Recently, Dutcher et al.<sup>19</sup> observed a shear-thinning effect (i.e., a decrease in the viscosity with the shear rate) during hole opening in freestanding PS thin films, showing that reptation is dominated by convective constraint release. More recently, some of us used the onset of the Plateau–Rayleigh instability of the rim observed during the dewetting of PS thin films to determine the transition between elastic and viscous regimes.<sup>39</sup> Interestingly, these transition times scale with  $\tau_{\text{rep}}$  of bulk PS, suggesting that bulk chain dynamics are maintained in thin films (even when  $h_0 < R_{\text{ee}}$  (the unperturbed end-to-end distance)).<sup>39</sup>

Such nanorheology experiments can be used to gain further insight into the structure and properties of out-of-equilibrium PS thin films. We may thus consider dewetting as a rheological probe to study the viscoelastic properties of nanoscopic polymer films, allowing us, for instance, to determine  $\tau_1$  of stressed materials (as discussed previously). In the following, we focus on the main parameters affecting the relaxation times of polymers and thus  $\tau_1$ : the chain length (represented by  $M_w$ ) and the temperature ( $T$ ). As shown in standard textbooks, the existence of entanglements implies that the longest relaxation times (i.e.,  $\tau_{\text{rep}}$ ) strongly depend on  $M_w$  according to a power law,  $\tau_{\text{rep}} \sim M_w^{3.4}$ .<sup>40,41</sup> It is also well known that, in polymeric materials, the temperature dependence of the relaxation time follows a non-Arrhenius behavior when  $T_g$  is approached. The thermal evolution of relaxation times is usually described by the Vogel–Tamman–Fulcher (VTF) relation:  $\tau = \tau_0 \exp[B/(T - T_0)]$ , where  $\tau_0$  is the segmental vibration frequency,  $B$  is 1170 K, and  $T_0$  is 343 K for bulk PS.<sup>40,41</sup>

As shown in Figure 6, the relaxation dynamics observed for spin-coated PS thin films drastically deviate from such bulk behavior. For instance, the dynamics slow down when the temperature decreases (i.e.,  $\tau_1$  increases). However, the ratio of relaxation times obtained from dewetting at 120 and 150 °C [Fig. 6(a)], given by  $\tau_1(120)/\tau_1(150) = 2.7$ , is

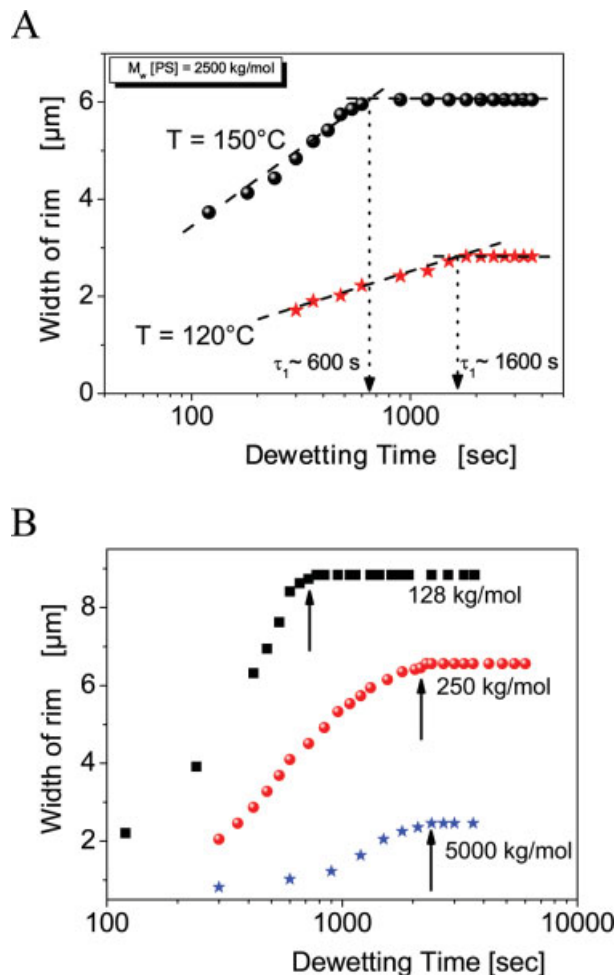


**Figure 6.** (A) Influence of the dewetting temperatures on  $\tau_1$  from plots of  $W$  versus time for PS thin films ( $h_0 = 40$  nm,  $M_w = 2500$  kD). The dewetting temperatures are indicated. (B) Influence of  $M_w$  on  $\tau_1$  from plots of  $W$  versus time for PS thin films ( $h_0 = 40$  nm, the dewetting temperature  $T_d = 125^\circ\text{C}$ ). The  $M_w$  values are indicated. [Color figure can be viewed in the online issue, which is available at [www.interscience.wiley.com](http://www.interscience.wiley.com).]

by more than 2 orders of magnitude lower than the ratio of the bulk viscosities,  $\eta(120)/\eta(150) = 500$  (computed from the VTF relation). The evolution of  $\tau_1$  with the molecular weight also shows striking deviations from bulk behavior. For high molecular weights, we observe that  $\tau_1$ , as determined from  $W_{\text{max}}$ -time plots, becomes independent of the chain length [Fig. 6(b)].

The observed  $\tau_1$  values are much shorter than the bulk  $\tau_{\text{rep}}$  values. In contrast with previous studies on hole opening in freestanding PS films,<sup>19</sup> we cannot invoke a convective constraint release effect (shear thinning) to account for the observed

decrease in the relaxation time. Indeed, because of the very high  $b$  values ( $b > h_0$ ), the velocity profile corresponds to a plug flow. Thus, the shear rates in our experiments are rather small (i.e., much smaller than  $\tau_{\text{rep}}^{-1}$ ). We emphasize, however, that we have no definite explanation for these unexpected results of extremely low temperature and molecular weight dependence for  $\tau_1$ . However, these observations lead us to ask the following fundamental questions: What is the nature of the out-of-equilibrium conformations of the spin-coated polymer films? What is the influence of confinement of chains on relaxation dynamics? Investigations of these aspects, highly relevant for a comprehensive understanding of dewetting and chain dynamics in thin films, are actively in progress and will be the subject of a forthcoming article.

## CONCLUSIONS

With both experimental and theoretical approaches, we have shown that the early stages of dewetting for spin-coated viscoelastic thin polymer films are dominated by the residual stresses and nonlinear friction at the solid/fluid interface. The residual stresses clearly result from the way in which these films are prepared, that is, by fast evaporation of the solvent during spin coating. As a result, depending on the preparation conditions, thermal history, and  $t_{\text{aging}}$  values, polymer thin films are formed by chains having more or less out-of-equilibrium conformations. Therefore, such films exhibit significant changes in their rupture probability, the dewetting dynamics, and various relaxation processes. The influence of the aging temperature, molecular weight, and dewetting temperature on these relaxation processes will be the subject of further studies.

This work was supported by the Belgian National Fund for Scientific Research, the Research Ministry of the Walloon Region (research project CORONET), and the Social European Fund. Both teams from France acknowledge financial support from the European Community's Marie-Curie Actions under contract MRTN-CT-2004-504052 (POLYFILM). P. Damman is a research associate of the Belgian National Fund for Scientific Research.

## REFERENCES AND NOTES

- de Gennes, P.-G.; Brochard-Wyart, F.; Quéré, D. *Capillarity and Wetting Phenomena: Drops, Bubbles, Pearls, Waves*; Springer: New York, 2003.



2. Cerda, E.; Ravi-Chandar, K.; Mahadevan, L. *Nature* 2002, 419, 579.
3. Alcoutlabi, M.; McKenna, G. B. *J Phys: Condens Matter* 2005, 17, R461.
4. Roth, C. B.; Dutcher, J. R. *Electroanal Chem* 2005, 584, 13.
5. Forrest, J. A.; Dalnoki-Veress, K. *Adv Colloid Interface Sci* 2001, 94, 167.
6. Reiter, G.; Hamieh, M.; Damman, P.; Sclavons, S.; Gabriele, S.; Vilmin, T.; Raphaël, E. *Nat Mater* 2005, 4, 754.
7. Croll, S. G. *J Appl Polym Sci* 1979, 23, 847.
8. Reiter, G.; de Gennes, P.-G. *Eur Phys J E* 2001, 6, 25.
9. Brochard-Wyart, F.; Redon, C. *Langmuir* 1992, 8, 2324.
10. Reiter, G.; Sharma, A. *Phys Rev Lett* 2001, 87, 166103.
11. Redon, C.; Brochard-Wyart, F.; Rondelez, F. *Phys Rev Lett* 1991, 66, 715.
12. Redon, C.; Brzoka, J. B.; Brochard-Wyart, F. *Macromolecules* 1994, 27, 468.
13. Brochard-Wyart, F.; Debrégeas, G.; Fondécave, R.; Martin, P. *Macromolecules* 1997, 30, 1211.
14. de Gennes, P. G. *Rev Mod Phys* 1985, 57, 827.
15. Brochard-Wyart, F.; Martin, P.; Redon, C. *Langmuir* 1993, 9, 3682.
16. (a) Reiter, G.; Khanna, R. *Phys Rev Lett* 2000, 85, 2753; (b) Reiter, G.; Khanna, R. *Langmuir* 2000, 16, 6351.
17. Debrégeas, G.; de Gennes, P. G.; Brochard-Wyart, F. *Science* 1998, 279, 1704.
18. Dalnoki-Veress, K.; Nickel, B. G.; Roth, C.; Dutcher, J. R. *Phys Rev E* 1999, 59, 2153.
19. Roth, C. B.; Deh, B.; Nickel, B. G.; Dutcher, J. R. *Phys Rev E* 2005, 72, 021802.
20. Podzimek, D.; Saier, A.; Seemann, R.; Jacobs, K.; Herminghaus, S. <http://arXiv:cond-mat/0105065 v1> (accessed May 2001).
21. Herminghaus, S.; Jacobs, K.; Mecke, K.; Bischof, J.; Fery, A.; Ibn-Elhaj, M.; Schlagowski, S. *Science* 1998, 282, 916.
22. Jacobs, K.; Seemann, R.; Mecke, K. In *Statistical Physics and Spatial Statistics*; Mecke, K.; Stoyan, D., Eds.; Springer: Heidelberg, 2000.
23. Reiter, G. *Phys Rev Lett* 1992, 68, 75.
24. Vrij, A. *Discuss Faraday Soc* 1966, 42, 23.
25. Konnur, R.; Kargupta, K.; Sharma, A. *Phys Rev Lett* 2000, 84, 931.
26. Reiter, G. *Phys Rev Lett* 2001, 87, 186101.
27. Damman, P.; Baudelet, N.; Reiter, G. *Phys Rev Lett* 2003, 91, 216101.
28. Herminghaus, S.; Seemann, R.; Jacobs, K. *Phys Rev Lett* 2002, 89, 056101.
29. Saulnier, F.; Raphaël, E.; de Gennes, P. G. *Phys Rev Lett* 2002, 88, 196101.
30. Shenoy, V.; Sharma, A. *Phys Rev Lett* 2002, 88, 236101.
31. Vilmin, T.; Raphaël, E. *Europhys Lett* 2005, 72, 781.
32. Rauscher, M.; Münch, A.; Wagner, B.; Blossey, R. *Eur Phys J E* 2005, 17, 373.
33. Bird, R. B.; Armstrong, R. C.; Hassager, O. *Dynamics of Polymeric Liquids*; Wiley: New York, 1977; Vol. 1.
34. Bureau, L.; Léger, L. *Langmuir* 2004, 20, 4523.
35. Casoli, A.; Brendlé, M.; Schultz, J.; Auroy, P.; Reiter, G. *Langmuir* 2001, 17, 388.
36. Vilmin, T.; Raphaël, E.; Damman, P.; Sclavons, S.; Gabriele, S.; Hamieh, M.; Reiter, G. *Europhys Lett* 2006, 73, 906.
37. Xavier, J. H.; Pu, Y.; Li, C.; Rafailovich, M. H.; Sokolov, J. *Macromolecules* 2004, 37, 1470.
38. Masson, J. L.; Green, P. F. *Phys Rev E* 2002, 65, 031806.
39. Gabriele, S.; Sclavons, S.; Reiter, G.; Damman, P. *Phys Rev Lett* 2006, 96, 156105.
40. De Gennes, P. G. *Scaling Concepts in Polymer Physics*; Cornell University Press: Ithaca, NY, 1979.
41. Rubinstein, M.; Colby, R. H. *Polymer Physics*; Oxford University Press: Oxford, 2003.